

Article

Torque Coordination Control during Braking Mode Switch for a Plug-in Hybrid Electric Vehicle

Yang Yang ^{1,2,*}, Chao Wang ², Quanrang Zhang ² and Xiaolong He ²¹ State Key Laboratory of Mechanical Transmission, Chongqing University, Chongqing 400044, China² School of Automotive Engineering, Chongqing University, Chongqing 400044, China; cqu_wang@163.com (C.W.); zqrguodu@163.com (Q.Z.); 13220343468@163.com (X.H.)

* Correspondence: yangyang@cqu.edu.cn; Tel.: +86-136-0831-1819

Received: 15 September 2017; Accepted: 16 October 2017; Published: 25 October 2017

Abstract: Hybrid vehicles usually have several braking systems, and braking mode switches are significant events during braking. It is difficult to coordinate torque fluctuations caused by mode switches because the dynamic characteristics of braking systems are different. In this study, a new type of plug-in hybrid vehicle is taken as the research object, and braking mode switches are divided into two types. The control strategy of type one is achieved by controlling the change rates of clutch hold-down and motor braking forces. The control strategy of type two is achieved by simultaneously changing the target braking torque during different mode switch stages and controlling the motor to participate in active coordination control. Finally, the torque coordination control strategy is modeled in MATLAB/Simulink, and the results show that the proposed control strategy has a good effect in reducing the braking torque fluctuation and vehicle shocks during braking mode switches.

Keywords: Hybrid Electric Vehicle (HEV); braking; mode switch; coordinated control; ride comfort

1. Introduction

Hybrid electric vehicles (HEVs) have attracted significant research attention because they can effectively reduce fuel consumption and emissions [1–3]. HEVs usually have several braking systems such as hydraulic and motor braking systems. Hydraulic braking systems can provide a stable and efficient braking force for a vehicle, and motor braking systems make energy recovery possible, thus expanding the driving range. Engine braking systems, which use engine drag resistance force during braking, can reduce the wear on a hydraulic braking system, thus saving maintenance expenses [4,5]. There are several braking modes during braking because of the existence of different braking systems. The different dynamic characteristics of hydraulic, motor, and engine braking systems cause torque fluctuations during braking mode switch, which deteriorates the riding comfort and the vehicle safety.

Currently, existing research on mode switching is mostly concentrated with the driving and less on the braking mode switch [6–8]. Zhang of Ji Lin University adopted a hierarchical control strategy in braking mode switches, then he designed a coordinated controller, based on a forward-feedback algorithm, to control the pneumatic braking system in order to compensate for errors of the motor braking force [9]. Fu of Tsinghua University analyzed the dynamic characteristics of the motor and the electronic vacuum booster (EVB) of a hybrid vehicle. The braking modes were divided into economic braking mode, safe braking mode with low state of charge (SOC), and safe braking mode with high SOC. Based on expected braking torque predictions, he proposed an electro-hydraulic coordinated braking control strategy [10]. Zhu of Tongji University designed a brake force distribution correction module and a motor force compensation module for transition conditions. These included hydraulic brake force intervention conditions, hydraulic brake force evacuation conditions, and regenerative brake force evacuation conditions with low speed. Those studies investigated the coordination control

between the motor and the mechanical braking system [11]. However, they did not make full use of the dynamic characteristics of the hydraulic, motor, and engine braking systems.

In this study, a new type of plug-in hybrid vehicle is taken as the research object, and the braking force distribution control strategy, which involves the engine drag resistance force, is developed. It is well known that the dynamic response of hydraulic braking systems is slow and stable, while the response of motor braking systems is fast and accurate [12]. The control strategy uses the hydraulic braking system to provide the required braking force, the motor to coordinate torque fluctuation, and the clutch to coordinate the engine drag force as a response to the problems of torque fluctuation during braking mode switch.

2. HEV Structure and Dynamic Model

2.1. HEV Structure

The structure of a plug-in hybrid vehicle, as shown in Figure 1, mainly includes an engine, an ISG motor, a permanent magnet synchronous motor (PMSM), a dual clutch, and an infinitely variable transmission (CVT). The front axle is driven by the engine and the integrated starter generator (ISG), the rear axle is driven by the PMSM, and the dual clutch is mounted on both ends of the ISG motor.

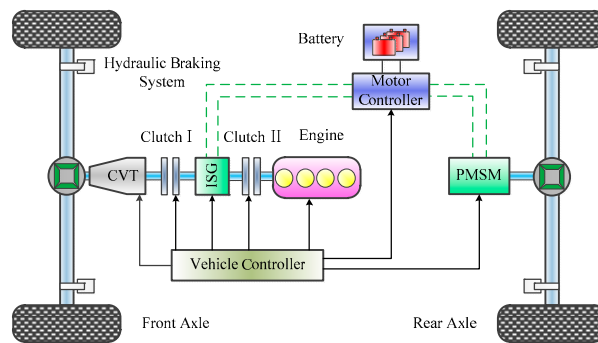


Figure 1. Structure of a plug-in hybrid vehicle.

2.2. Dynamic Model

2.2.1. Motor Dynamic Model

The three-phase PMSM is a strongly coupled and multivariable nonlinear system [13]. In order to accurately reflect the dynamic response characteristics of the motor during braking, a dynamic model is established based on the mathematical model of the three-phase PMSM. In the synchronous rotating coordinate system (d - q axis), the ideal PMSM voltage equation [14] is:

$$\begin{cases} u_d = Ri_d + L_d \frac{d}{dt} i_d - \omega_e L_q i_q \\ u_q = Ri_q + L_q \frac{d}{dt} i_q + \omega_e (L_d i_d + \psi_f) \end{cases} \quad (1)$$

The electromagnetic torque equation is:

$$T_e = \frac{3}{2} p_n i_q [i_d (L_d - L_q) + \psi_f] \quad (2)$$

where u_d , u_q respectively represent the stator voltage d - q axis component; i_d , i_q respectively represent the stator current d - q axis component; R is stator resistance; ω_e is electrical angular velocity; L_d , L_q respectively represent inductance d - q axis component; ψ_f is permanent magnet flux chain; p_n is motor pole pairs.

2.2.2. Hydraulic Dynamic Model

The dynamic response characteristics of the hydraulic braking system are related to the hydraulic system structural parameters, duty cycle and so on. However, building a precise model of the hydraulic braking system is difficult and the required computational power is large. In order to simplify the model and accurately reflect the dynamic characteristics of the hydraulic system, this study uses the empirical first-order inertia link [15]:

$$\begin{cases} T_{hf} = P_f \frac{1}{4} \pi D_f^2 R_f B_{Ff} \frac{1}{s\tau + 1} \\ T_{hr} = P_r \frac{1}{4} \pi D_r^2 R_r B_{Fr} \frac{1}{s\tau + 1} \end{cases} \quad (3)$$

where T_{hf} , T_{hr} are the front and rear axle brake torque; P_f , P_r are cylinder pressures; D_f , D_r are axle cylinder diameter; R_f , R_r are brake operating radius; B_{Ff} , B_{Fr} are brake efficiency factors; τ is the first-order system time constant, which can be obtained by experience; s is a variable.

As shown in Figure 2, the motor torque response is quick and accurate, the response time is approximately 0.06 s, and the overshoot is 11.12%. Compared with the motor, in order to overcome the brake clearance and cylinder pressurization, the hydraulic system's torque response is slow but stable and the response time is approximately 0.17 s. According to [16], the full starting time of the driving brake is generally controlled within 0.2–0.3 s; thus, the dynamic response characteristics of the hydraulic model constructed in this study satisfies this requirement.

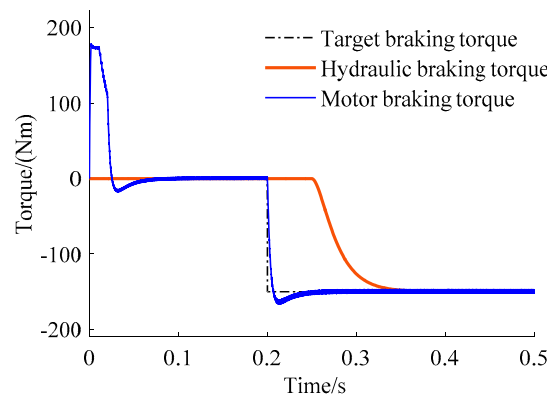


Figure 2. Step response of motor and hydraulic braking torque.

2.2.3. Engine Drag Model

When the engine is anti-dragged, the throttle is closed and the engine drag resistant torque is related to the engine speed, as shown in Figure 3. Because the engine has multiple subsystem modules, the establishment of the engine model is difficult. At the same time, this study does not consider the problem of engine emissions. Therefore, this study uses the experimental modeling method to establish the engine model, and the output response of the engine drag resistant torque is characterized by a second-order transfer function:

$$T_{bICE} = \frac{\omega_n^2}{s^2 + 2\zeta\omega_n s + \omega_n^2} f(n_e) \quad (4)$$

where ω_n is the natural frequency; ζ is the damping coefficient; n_e is the engine speed; T_{bICE} is the engine drag resistant torque; s is a variable.

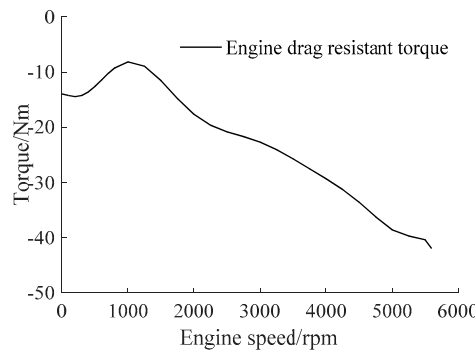


Figure 3. Engine drag resistance torque.

3. Braking Force Distribution Strategy

The hybrid electric vehicle mentioned above is equipped with dual motors, and during braking, the maximum strength of the motor brake ranges from 0.06 to 0.27 with the speed and CVT ratio changing. Therefore, in order to recover as much energy as possible, this study puts forward a brake force distribution strategy based on the motor braking capacity, while taking the engine brake into consideration.

The braking force distribution curve is shown in Figure 4. V is the speed of the vehicle; V_{max} and V_{min} are the maximum and minimum vehicle speeds allowed for regenerative braking; SOC_{high} is the maximum state of charge allowed for regenerative braking; i_{o1} and i_{o2} are the transmission ratios of final drive I and final drive II; i_{cvt} is the CVT transmission ratio; z is the braking strength; F_{b_req} is the total braking force the driver demanded; F_{bm_req} , F_{bh_req} and F_{bICE_req} are the target motor, hydraulic and engine braking forces; F_{bxf_req} and F_{bxx_req} are the target braking forces of the front and rear axles of the vehicle; F_{blhf_req} and F_{blhr_req} are the target hydraulic braking forces of the front and rear axles; F_{bI_req} and F_{bP_req} are the target braking forces of ISG and PMSM; F_{bI_max} and F_{bP_max} are the maximum braking forces that ISG and PMSM can provide in the current state; F_{bICE} is the engine drag resistant force; F_{bm_max} is the maximum braking force that the motor can provide; β is the ratio between front axle and total braking force.

As seen in Figure 4, the point E is the intersection of line $z = 0.4$ and curve I while the point F is the intersection of line $z = 0.7$ and curve I. Therefore, the β line consists of the OE and EF segments and the braking strengths of A, B and C are:

$$\begin{cases} z(A) = \frac{i_{o2}F_{bP_max}}{G} \\ z(B) = \frac{F_{bm_max}}{G} \\ z(C) = \frac{i_{o2}F_{bP_max}(1+\beta_1)}{G} \end{cases} \quad (5)$$

The required motor braking force is:

$$F_{bm_req} = i_{cvt}i_{o1}F_{bI_req} + i_{o2}F_{bP_req} \quad (6)$$

The required hydraulic braking force is:

$$F_{bh_req} = F_{bhf_req} + F_{bhr_req} \quad (7)$$

The required braking force is:

$$F_{b_req} = Gz \quad (8)$$

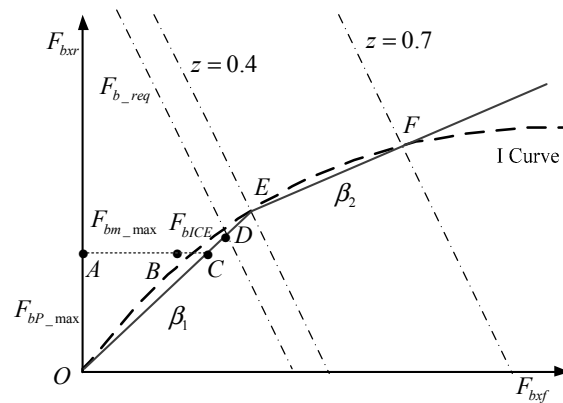


Figure 4. The braking force distribution curve. (F_{bxf}) Braking force in the front axle; (F_{bxr}) braking force in the rear axle; (I curve) the ideal braking force distribution curve.

The detailed braking force distribution strategies are as follows:

When $V_{min} < V < V_{max}$ and $SOC < SOC_{high}$:

(1) $0 < z \leq z(B)$

In this condition, braking force is completely provided by the regenerative braking force. $F_{bh_req} = 0$, $F_{bm_req} = F_{b_req}$. The braking forces of ISG and PMSM are distributed as follows:

When $0 < z \leq z(A)$,

$$\begin{cases} F_{bI_req} = 0 \\ F_{bP_req} = \frac{F_{b_req}}{i_{o2}} \end{cases} \quad (9)$$

When $z(A) < z \leq z(B)$,

$$\begin{cases} F_{bI_req} = \frac{F_{b_req} - i_{o2}F_{bP_max}}{i_{cvt}i_{o1}} \\ F_{bP_req} = F_{bP_max} \end{cases} \quad (10)$$

(2) $z(B) < z \leq z(C)$

In order to make full use of engine to brake, the braking force is provided by the motor and the engine braking system. Therefore, $F_{bh_req} = 0$, $F_{b_req} = F_{bm_req} + i_{cvt}i_{o1}F_{bICE}$.

$$\begin{cases} F_{bICE_req} = F_{bICE} \\ F_{bI_req} = \frac{F_{b_req} - i_{o2}F_{bP_max}}{i_{cvt}i_{o1}} - F_{bICE} \\ F_{bP_req} = F_{bP_max} \end{cases} \quad (11)$$

(3) $z(C) < z \leq z(F)$

When $z(C) < z \leq z(F)$, the braking force is provided by the motor and the hydraulic braking system. The target braking forces of the front and rear axles, distributed in accordance with line CEF shown in Figure 4, are F_{bxf_req} and F_{bxr_req} . Therefore, $F_{bICE} = 0$, $F_{b_req} = F_{bm_req} + F_{bh_req}$. The braking forces of the motor and hydraulic braking system are:

$$\begin{cases} F_{bI_req} = F_{bI_max} \\ F_{bP_req} = F_{bP_max} \\ F_{bh_req} = F_{bxf_req} - i_{cvt}i_{o1}F_{bI_max} \\ F_{bhr_req} = F_{bxr_req} - i_{o2}F_{bP_max} \end{cases} \quad (12)$$

When $V > V_{max}$ or $V < V_{min}$ or $SOC \geq SOC_{high}$ or $z > z(F)$, the braking force is completely provided by the hydraulic braking system. The braking forces of the hydraulic braking system are:

$$\begin{cases} F_{bhf_req} = F_{bxf_req} \\ F_{bhr_req} = F_{bxr_req} \end{cases} \quad (13)$$

4. Coordinated Control Strategy for Braking Mode Switch

4.1. Kinetics Analysis of Braking Mode

According to the braking force distribution control strategy mentioned above, there are four main braking modes: pure electric braking mode, motor and engine braking mode, motor and hydraulic braking mode, and hydraulic braking mode. In order to facilitate the kinetic analysis, the hybrid vehicle drive system model is simplified, as illustrated in Figure 5.

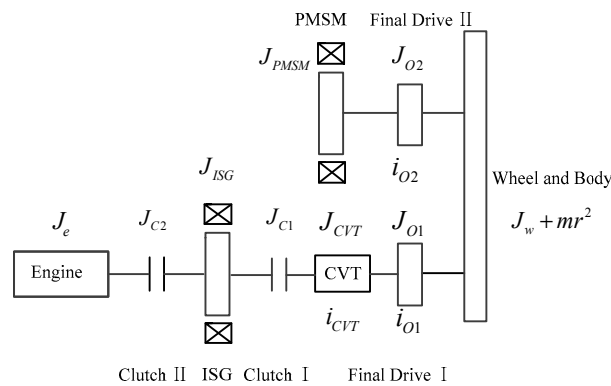


Figure 5. Equivalent diagram of the system model.

where J_e is moment of inertia of the engine; J_{ISG} is moment of inertia of the ISG; J_{cvt} is moment of inertia of the CVT; J_{C1} is moment of inertia of the clutch I; J_{C2} is moment of inertia of the clutch II; J_{PMSM} is moment of inertia of the PMSM; J_w is moment of inertia of the wheel; J_{O1} is moment of inertia of the final drive I; J_{O2} is moment of inertia of the final drive II; m is the vehicle mass; r is the tire radius.

(1) Pure Electric Braking Mode

When the motor is braking clutch I is engaged and clutch II is disconnected. The engine and the hydraulic braking systems do not participate in the braking action and the required braking torque is provided by the motor. The equivalent to the moment of inertia on the wheel is:

$$J_v = ((J_{ISG} + J_{C1}) \cdot i_{cvt} + J_{CVT}) \cdot i_{O1} + J_{O1} + J_{O2} + J_{PMSM} \cdot i_{O2} + J_w + mr^2 \quad (14)$$

The dynamic equation of braking is:

$$\begin{cases} T_{bICE} = 0 \\ T_{bh} = 0 \\ T_{bISG} \cdot i_{cvt} \cdot i_{O1} + T_{bPMSM} \cdot i_{O2} = J_v \dot{\omega}_w \end{cases} \quad (15)$$

where T_{bICE} is the engine drag resistance torque, T_{bh} is the hydraulic braking torque, T_{bISG} is the ISG braking torque, T_{bPMSM} is the PMSM braking torque, and $\dot{\omega}_w$ is the wheel angular acceleration.

(2) Motor and Engine Braking Mode

When the motor and engine are involved in braking, clutches I and II are engaged. The required braking torque is provided by the motor and the engine. At this time, the equivalent to the moment of inertia on the wheel is:

$$J_v = ((J_e + J_{ISG} + J_{C1} + J_{C2}) \cdot i_{cvt} + J_{CVT}) \cdot i_{O1} + J_{O1} + J_{O2} + J_{PMSM} \cdot i_{O2} + J_w + mr^2 \quad (16)$$

The dynamic equation of braking is:

$$\begin{cases} T_{bh} = 0 \\ (T_{bISG} + T_{bICE}) \cdot i_{cvt} \cdot i_{O1} + T_{bPMSM} \cdot i_{O2} = J_v \dot{\omega}_w \end{cases} \quad (17)$$

(3) Motor and Hydraulic Braking Mode

During motor and hydraulic braking modes, clutch I is engaged and clutch II is disconnected. The required braking torque is provided by the motor and the hydraulic braking system. At this time, the equivalent to the moment of inertia on the wheel is:

$$J_v = ((J_{ISG} + J_{C2}) \cdot i_{cvt} + J_{CVT}) \cdot i_{O1} + J_{O1} + J_{O2} + J_{PMSM} \cdot i_{O2} + J_w + mr^2 \quad (18)$$

The dynamic equation of braking is:

$$\begin{cases} T_{bICE} = 0 \\ T_{bISG} \cdot i_{cvt} \cdot i_{O1} + T_{bPMSM} \cdot i_{O2} + T_{bh} = J_v \dot{\omega}_w \end{cases} \quad (19)$$

(4) Hydraulic Braking Mode

During hydraulic braking mode, clutches I and II are disengaged and the required braking torque is provided by the hydraulic braking system. The equivalent to the moment of inertia on the wheel is:

$$J_v = J_{CVT} \cdot i_{O1} + J_{O1} + J_{O2} + J_{PMSM} \cdot i_{O2} + J_w + mr^2 \quad (20)$$

The dynamic equation of braking is:

$$\begin{cases} T_{bICE} = 0 \\ T_{bISG} = T_{bPMSM} = 0 \\ T_{bh} = J_v \dot{\omega}_w \end{cases} \quad (21)$$

Based on the kinetics analysis of the braking mode, there are three types of braking torque that need to be coordinated during braking mode switching. The motor, the hydraulic, and the engine braking systems are three different systems with different dynamic response characteristics; therefore, the sequences and moments of the three joint systems are different. Because mode switching is completed instantaneously, the braking torque varies sharply during the intervention and exit from braking. If there is no coordinated control, it will cause torque fluctuation and seriously worsen the ride comfort of the vehicle.

4.2. Coordination Control Strategy for Mode Switch

According to whether or not the hydraulic braking system is involved in braking, the braking mode-switch type is divided into two categories (Figure 6). Braking mode-switch coordination control strategies are developed for the different braking mode-switch types.

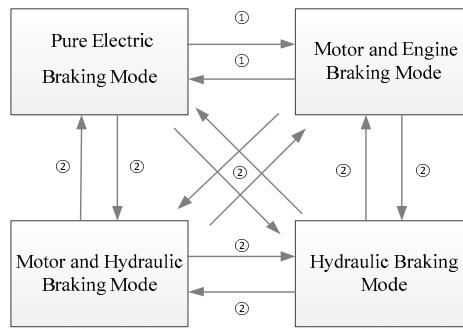


Figure 6. Braking mode switch classification.

(1) Type one: braking mode switch without hydraulic braking system participation. In this type of mode switching it is necessary to control the engagement of the clutch and the change rate of the motor torque. Thus, the fluctuation caused by mode switch can be reduced.

(2) Type two: braking mode switch with hydraulic braking system participation. Due to the different dynamic response characteristics of the motor and the hydraulic braking systems, this switch mode is difficult to coordinate. The idea of coordinating control is to take full advantage of the characteristics of the braking systems. The hydraulic system can provide large and stable torque, and the motor braking system's torque response is quick and accurate, reducing the fluctuation of the vehicle.

The overall coordination control flow chart is shown in Figure 7. T_{bm_req} , T_{bh_req} and T_{bICE_req} are the target motor, hydraulic and engine braking torques allocated by the braking force control strategy.

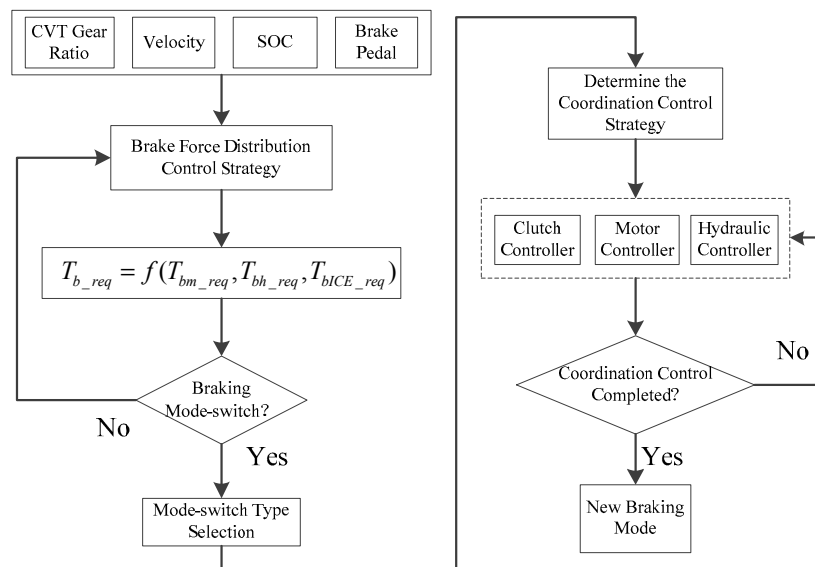


Figure 7. Flow chart of overall coordination control.

First, according to current speed, SOC, CVT ratio, and brake pedal, the braking force distribution control strategy allocates the target motor, hydraulic and engine braking torques; then, according to the braking mode boundary conditions the vehicle controller determines whether the braking mode should switch or not. If mode switching happens, the vehicle controller determines the type of mode switch and then selects the corresponding coordination control strategy and controls the clutch, motor and hydraulic torques to reduce the mode switch fluctuation. Finally, the vehicle controller determines whether the coordination control is completed, and if it is completed, the vehicle will enter a new braking mode.

4.2.1. Coordination Control Strategy of Type One

In this type of mode switch the motor braking torque and the engine drag resistance torque, transmitted by clutch II, are the main sources of braking torque fluctuation. Therefore, the braking torque fluctuation is coordinated by controlling the change rate of the clutch hold-down force and the motor brake force. The torque transmitted by the dry clutch during slipping is:

$$T_c = \text{sign}(\Delta\omega) \frac{2}{3} \mu F(t) Z \frac{R_0^3 - R_1^3}{R_0^2 - R_1^2} \quad (22)$$

where $\Delta\omega$ is the clutch angular velocity difference between the main and driven plate; sign is symbolic function; μ is clutch friction factor, which is related to the surface temperature of the plates and $\Delta\omega$; $F(t)$ is the compression force of clutch plates; Z is the clutch friction pair number; R_0, R_1 are the clutch outer and inner friction plate diameter.

The coordinated control flow chart of type one is shown in Figure 8, k_m and k_c are the change rates of motor brake torque and clutch hold-down force. T_{bm} and T_c are the actual torques of motor and clutch and $T_{bm} = T_{bISG}i_{cvt}i_{o1} + T_{bPMSM}i_{o2}$. T_b is the actual total brake torque.

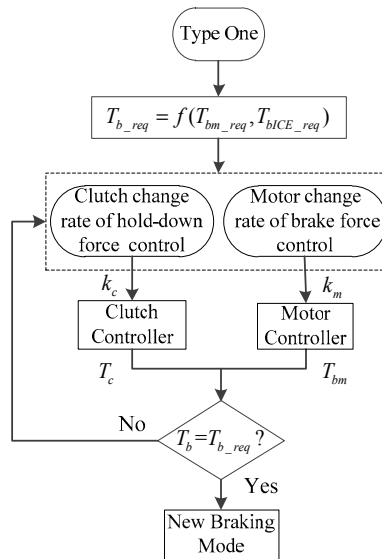


Figure 8. Flow control chart of the first type mode-switch.

It is simple to control the motor brake force changing rate, however, it is hard to obtain the target change rate of the clutch hold-down force. Moreover, it is assumed that the target change rate of the total brake force is k_{req} . Thus:

$$\begin{cases} F(t) = F_0 + \int k_c dt \\ T_{bm}(t) = T_{bm0} + \int k_m dt \\ T_b(t) = T_{b0} + \int k_{req} dt \end{cases} \quad (23)$$

where F_0, T_{bm0} and T_{b0} are the initial values of the clutch hold-down force, the motor brake torque, and the total brake force.

Then:

$$T_b(t) = T_{bm}(t) + T_c i_{cvt} i_{o1} \quad (24)$$

Derivation of the formula above gives:

$$k_{req} = k_m + a i_{cvt} i_{o1} k_c \quad (25)$$

and:

$$a = \text{sign}(\Delta\omega)\mu ZR \quad (26)$$

Therefore, the change rate of clutch hold-down force is:

$$k_c = \frac{k_{req} - k_m}{a i_{cvt} i_{o1}} \quad (27)$$

4.2.2. Coordination Control Strategy of Type Two

The dynamic response of the hydraulic braking system is slow and stable while the response of the motor braking system is fast and accurate. The hydraulic brake system has been developed for a long time, its technology is mature and stable, and its dynamic response characteristics have been well researched [17]. Therefore, in order to make full use of the characteristics of the motor and the hydraulic braking systems, the coordinated control process of braking mode switch is divided into two stages; this is achieved by modifying the target braking torque.

The coordinated control flow chart of type two is shown in Figure 9, T_{bm}' , T_{bh}' and T_{bICE}' are the modified target braking torques of the motor, the hydraulic and the engine braking system; T_{bm0} , T_{bh0} and T_{bICE0} are the initial torques of the motor, the hydraulic and the engine braking system when mode is switched; T_c is the transmitted torque of the dry clutch. When mode switch happens, the coordination control process is described as follows: during mode switching, the torques of the motor, the hydraulic and the engine braking system are:

$$\begin{cases} T_{bm} = T_{bm0} \\ T_{bh} = T_{bh0} \\ T_{bICE} = T_{bICE0} \end{cases} \quad (28)$$

At that moment, the coordinated control process of the braking mode switch enters into the first stage: it keeps the brake torques of the motor and engine unchanged and modifies the target braking torque of the hydraulic braking system to meet the driver demand. Therefore, the modified torques are:

$$\begin{cases} T_{bm}' = T_{bm0} \\ T_{bh}' = T_{b_req} - T_{bm0} - i_{cvt} i_{o1} T_{bICE0} \\ T_{bICE}' = T_{bICE0} \end{cases} \quad (29)$$

Next, the vehicle controller determines whether T_b is equal to T_{b_req} , if $T_b = T_{b_req}$, the coordinated control process enters into the second stage: it makes full use of the dynamic characteristics of the motor braking system to coordinate the torque fluctuation and modifies the target braking torque of the engine and the hydraulic braking system in order to reach the target value (T_{bh_req} and T_{bICE_req})

$$\begin{cases} T_{bm}' = T_{b_req} - T_{bh} - i_{cvt} i_{o1} T_c \\ T_{bh}' = T_{bh_req} \\ T_{bICE}' = T_{bICE_req} \end{cases} \quad (30)$$

Finally, the vehicle controller evaluates whether $T_{bm} = T_{bm_req}$ and $T_{bICE} = T_{bICE_req}$ if so, the current mode is substituted by a new braking mode.

A motor torque proportional-integral-derivative (PID) control algorithm was designed in order to improve the hydraulic and clutch torque fluctuation and keep the total braking torque stable during the second stage. The PID algorithm's control structure is shown in Figure 10. The input is T_{bm}' which

is the modified target braking torque of the motor while the output is T_{bm} which is the actual braking torque of the motor.

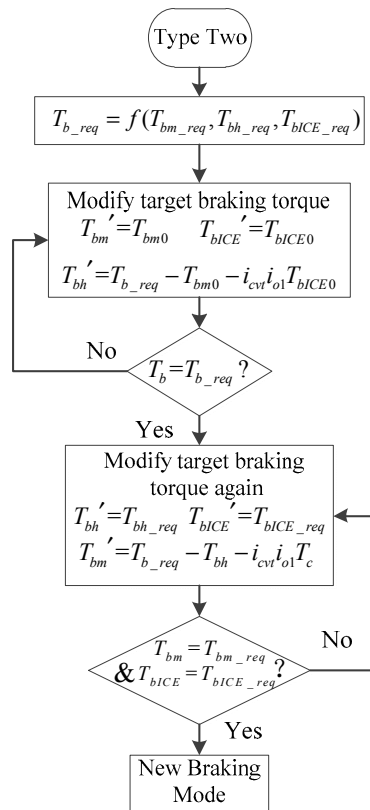


Figure 9. Flow control chart of the second type mode-switch.

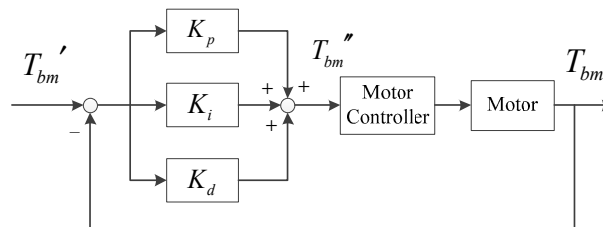


Figure 10. Motor torque PID control algorithm.

The PID control algorithm's expression is:

$$\begin{cases} T_{bm}'' = K_p e(t) + K_i \int e(t) dt + K_d \frac{d}{dt} e(t) \\ e(t) = T_{bm}' - T_{bm} \end{cases} \quad (31)$$

where $e(t)$ is the PID deviation; K_p , K_i and K_d are the PID ratio, the integral and the differential factors.

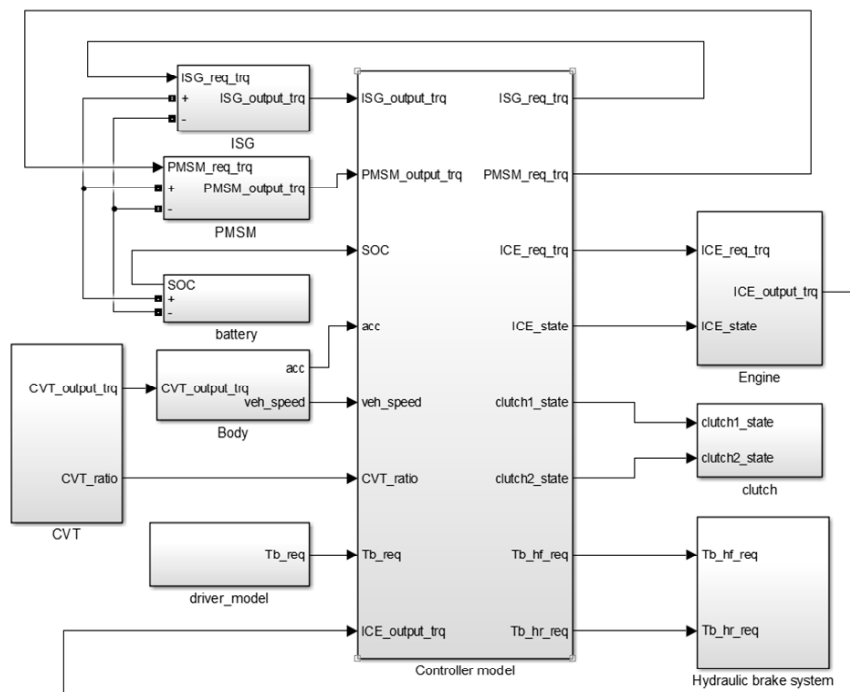
5. Simulation Results and Analysis

In this study, the simulation model of a plug-in four-wheel drive hybrid vehicle was established on the MATLAB/Simulink simulation platform. The parameters of the hybrid vehicle and the key components are listed in Table 1. The effectiveness of the coordinated control strategy was studied by comparing the results with and without a control strategy. In the simulation of the non-coordinated control strategy, motor, hydraulic and clutch torques are not intervened during the braking mode switch while the other parameters remained the same.

Table 1. The parameters of vehicle and key components.

Components	Parameters	Value
Vehicle	Mass/kg	1800
Engine	Displacement/L	1.597
	Peak power/Kw	69
ISG	Peak power/Kw	28
PMSM	Peak power/Kw	27
Battery	Type of battery	Lithium

In this paper, the forward simulation model of plug-in hybrid vehicle is established based on MATLAB/Simulink, as illustrated in Figure 11. The vehicle simulation model is composed of ISG model, PMSM model, battery model, hydraulic braking system model and the controller model.

**Figure 11.** Vehicle simulation model based on Simulink.

The hybrid vehicle's brake mode-switch types in this study are complex and numerous and it would require a lot of computational power for the simulation analysis of each brake mode switch. Therefore, this study simulated several typical braking mode-switch conditions to verify the effectiveness of the coordinated control strategy. The typical braking mode-switch conditions were as follows: (1) motor braking mode to motor and engine braking mode; (2) motor braking mode to motor and hydraulic braking mode; (3) motor and engine braking mode to motor and hydraulic braking mode; (4) motor and hydraulic braking mode to hydraulic braking mode. This paper takes the urgent situation into consideration, therefore, the step type of target braking force is set, and the simulation results were as follows: when the vehicle speed was 60 km/h and the braking strength was changed from 0.05 to 0.2, the braking mode was switched, at 0.2 s, from the motor brake to the motor and engine brake (Figure 12). In the model without coordination the motor quickly reached the target braking torque due to its rapid response characteristics. The dramatic change of the motor torque had a great impact on the ride comfort of the vehicle, the vehicle jerk caused by the motor reached 86.06 m/s^3 . Because the clutch was engaged in a slower time than the motor response, it took longer

time for it to reach the target value. In the model with coordination, due to fact that the change rate of the motor was limited, the impact caused by the motor torque was significantly improved and the value of vehicle jerk was less than 15.18 m/s^3 . Therefore, the coordinated control strategy significantly improved the vehicle's ride comfort.

As shown in Figure 13, when the braking strength is changed from 0.1 to 0.3, the braking mode is switched from the motor brake to the motor and hydraulic brake. In the results without coordination the hydraulic system response was slower and the hydraulic braking system reached the target braking torque after the motor, therefore, it had a large impact on the vehicle. In the results with coordination the vehicle fluctuation was significantly improved by coordinating the motor and the hydraulic braking torque. However, a small fluctuation occurred at 0.42 s because the motor did not have enough ability to coordinate the change of the hydraulic braking torque. The jerk of a small fluctuation was less than 1.57 m/s^3 and the effect of the coordinated control is pretty good.

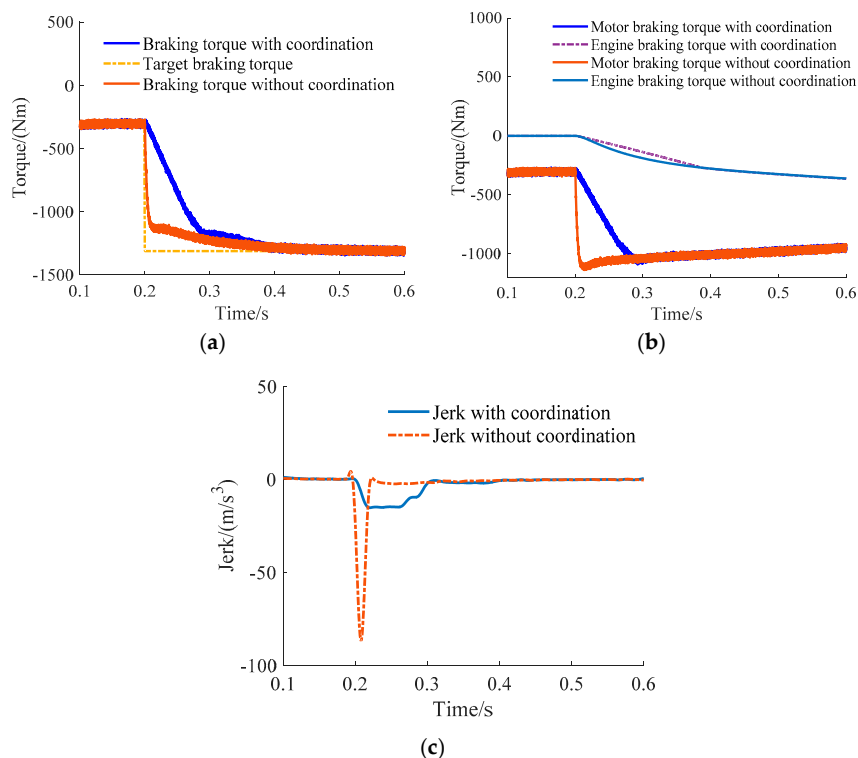


Figure 12. Simulation results of motor braking mode to motor and engine braking mode. (a) Total braking torque; (b) Motor and engine braking torque; (c) Vehicle jerk.

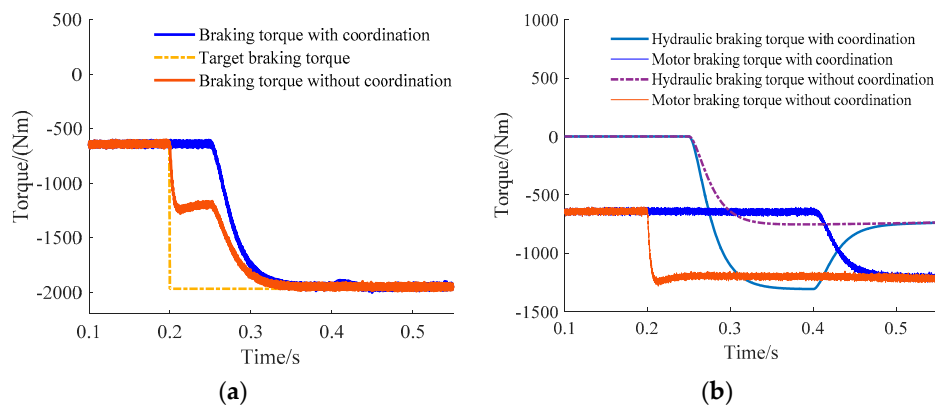


Figure 13. Cont.

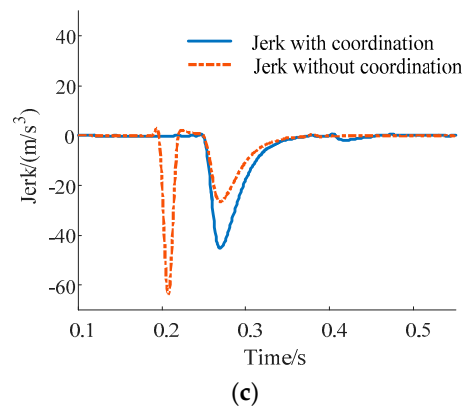


Figure 13. Simulation results of motor braking mode to motor and hydraulic braking mode. (a) Total braking torque; (b) Motor and hydraulic braking torque; (c) Vehicle jerk.

Figure 14 shows that the braking mode changes from motor and engine brake to motor and hydraulic brake. During mode switch, the engine exits the anti-drag brake, and the hydraulic system is involved in braking. Figure 14a shows that the total braking torque fluctuation without coordination is very intense. Meanwhile, the torque fluctuation with coordination is smaller.

When the mode is switched from motor and hydraulic brake to hydraulic brake (Figure 15), the motor exits the regenerative brake mode, the motor braking torque drops suddenly and the hydraulic braking torque rises slowly. The vehicle jerk without coordination can reach 138.4 m/s^3 and the ride comfort is seriously worsened. However, the jerk with coordination is less than 95 m/s^3 .

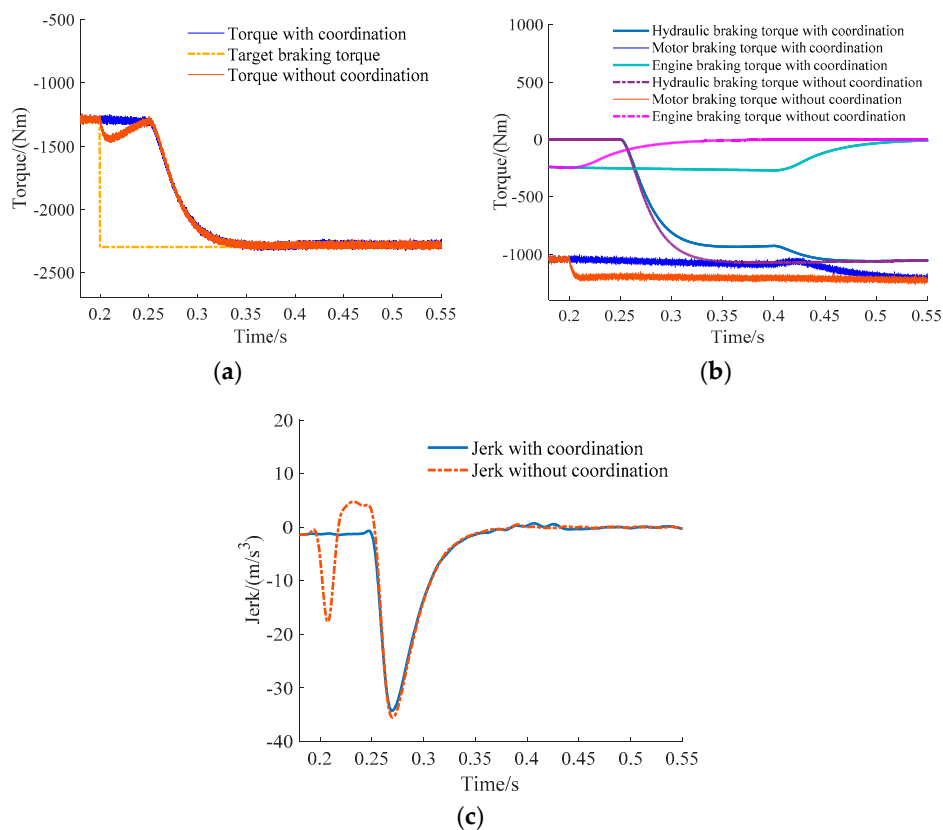


Figure 14. Simulation results of motor and engine braking mode to motor and hydraulic braking mode. (a) Total braking torque; (b) Motor, engine and hydraulic braking torque; (c) Vehicle jerk.

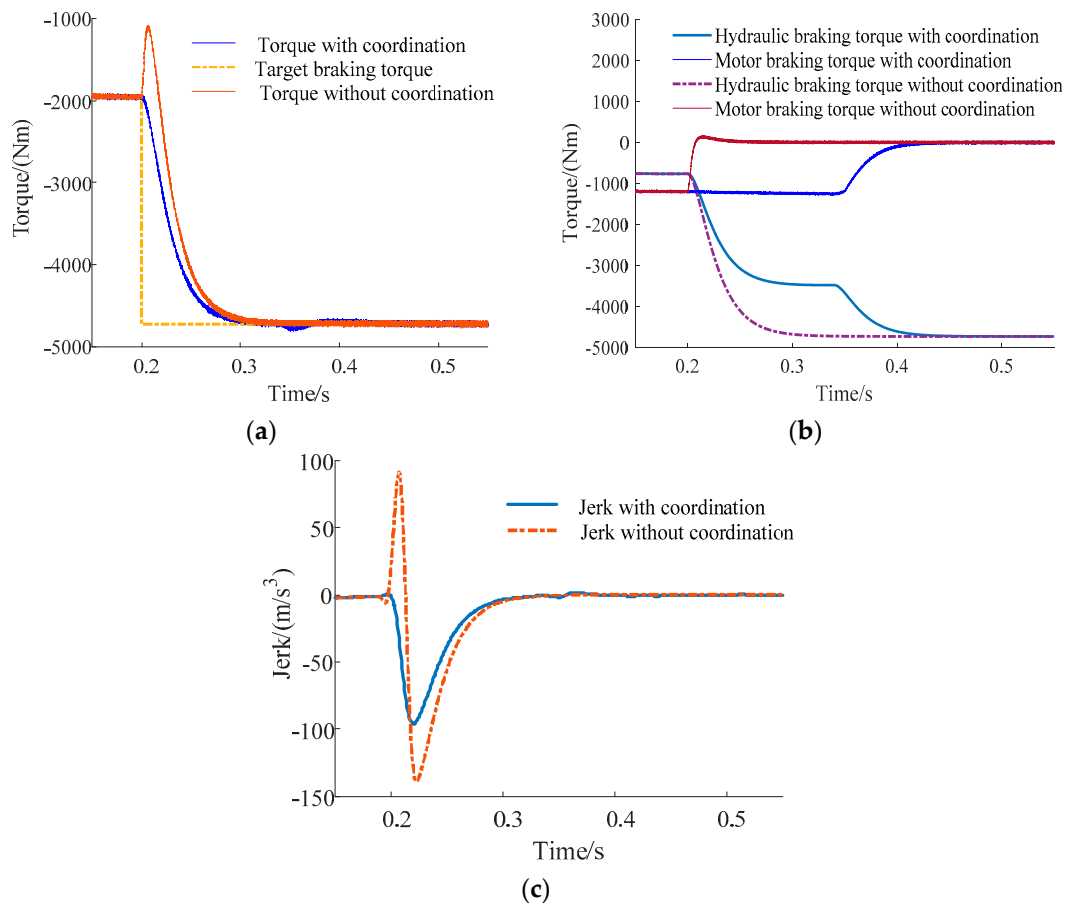


Figure 15. Simulation results of motor and hydraulic braking mode to hydraulic braking mode. (a) Total braking torque; (b) Motor and hydraulic braking torque; (c) Vehicle jerk.

6. Conclusions

In this study, a new type of plug-in hybrid was taken as the research object and the braking force distribution strategy which takes the engine drag resistance torque into consideration was put forward. The types of braking mode switches were divided into two types, aimed at the problem of torque fluctuation during the braking mode switch. Two coordinated control strategies which correspond to the two types were developed by analyzing the clutch and the characteristics of the hydraulic and the motor braking systems. The coordination control strategy of type one was achieved by controlling the change rates of the clutch hold-down force and the motor braking force. By comparing the characteristics of the motor and the hydraulic braking systems, it was found that the dynamic response of the hydraulic braking system is slow and stable, while the response of the motor braking system is fast and accurate. Therefore, the strategy of type two was coordinated by modifying the target braking torque during the braking mode switch. Meanwhile, control of the motor braking system was utilized to actively improve the torque fluctuation and a motor torque PID control algorithm was designed for this purpose. Finally, a coordination control strategy simulation was performed on the MATLAB/Simulink platform; the simulation results showed that the coordination control strategy can effectively reduce the vehicle jerk under specific road conditions during a typical braking mode switch. These promising results are meaningful for further research on the torque coordination of the braking mode switch.

Acknowledgments: The research is supported by: (1) the National Natural Science Foundation of China (51575063); (2) the Chongqing Significant Application and Development Planning Project (cstc2015yykfC60003).

The authors would also like to acknowledge the support from the State Key Laboratory of Mechanical Transmission of Chongqing University, China. The authors are indebted to the people who have helped to improve the paper.

Author Contributions: Yang Yang designed the structure of hybrid vehicle system and proposed the coordination control strategies; Chao Wang built the simulation model based on Simulink and acquired the simulation data. Xiaolong He and Quanrang Zhang participated in data processing.

Conflicts of Interest: The authors declare no conflict of interest.

References

1. Zhao, Z.; He, N.; Zhu, Y.; Yu, Z. Mode Transition Control for Four Wheel Drive Hybrid Electric Car. *J. Mech. Eng.* **2011**, *47*, 100–101. [[CrossRef](#)]
2. Kerem, K. Modeling and Control of a Hybrid-Electric Vehicle for Drivability and Fuel Economy Improvements. Ph.D. Thesis, Ohio State University, Columbus, OH, USA, May 2008.
3. Steven, M. Mechanical and Regenerative Braking Integration for a Hybrid Electric Vehicle. Ph.D. Thesis, University of Waterloo, Waterloo, ON, Canada, August 2008.
4. Zhang, J.; Lu, C.; Li, Y.; He, C. Status quo and prospect of regenerative braking technology in electric cars. *Automot. Eng.* **2014**, *36*, 911–917.
5. Zheng, Z. Research of Brake Pedal Stroke Simulator and Braking Smoothness Based on Electric-Wheel Vehicle. Ph.D. Thesis, Jilin University, Changchun, China, June 2013.
6. Korowais, K.; Westervelt, E.R.; Rizzoni, G. Toward the systematic Design of Controllers for Smooth Hybrid Electric Vehicle Mode Changes. In Proceedings of the 2007 American Control Conference, New York, NY, USA, 9–13 July 2007.
7. Yang, Y.; Huang, J.; Qin, D.; Duan, Z. Control Strategy for Operation Mode Switch of Dual-Clutch Hybrid Electric Vehicle. *Automot. Eng.* **2013**, *35*, 723–730.
8. Yang, Y.; Huang, J.; Qin, D.; Yang, W. Coordinated Torque Control for Model-switch between Motor and Engine Driving in Heavy Hybrid Electric Vehicle. *Appl. Mech. Mater.* **2011**, *86*, 779–783. [[CrossRef](#)]
9. Zhang, T. Study on the Coordination Control Algorithm of Braking Force for HEV Bus. Master's Thesis, Jilin University, Changchun, China, June 2011.
10. Fu, X.; Luo, Y.; Han, Y.; Jiang, F.; Li, K. Coordinated Control Strategy for the Electro-Hydraulic Braking System of Intelligent Hybrid Electric Vehicle. *Automot. Eng.* **2011**, *33*, 915–919.
11. Numasato, H.; Tomizuka, M. Settling Control and Performance of a Dual-Actuator. *IEEE/ASME Trans. Mech.* **2008**, *8*, 431–438. [[CrossRef](#)]
12. Wang, K.; He, R. Analysis on Coordination Control Technology of Electric-Mechanical Composite Braking System of Vehicle. *Nat. Sci.* **2014**, *12*, 10–17.
13. Yuan, L.; Hu, B.; Wei, K.; Chen, S. *Control Principle of Modern PMSM and Matlab Simulation*; Beijing University of Aeronautics and Astronautics Press: Beijing, China, 2016.
14. Jin, L.; Wang, X.; Li, W. Current Sliding Mode Control and Load Disturbance Compensation of PMSM for HEV. *Automot. Eng.* **2013**, *35*, 553–558.
15. Yang, Y.; Li, X.; Su, N.; Huang, J. Control Strategy for Mode-Switch of Full Hybrid Electric Vehicle. *China J. Highw. Transp.* **2014**, *27*, 109–119.
16. Gong, M.; Zhao, D.; Xu, M. Two-way Hydraulic Braking System Performance Simulation of Heavy Vehicles. *J. Jilin Univ. Technol.* **2010**, *40*, 725–728.
17. Wu, T. Study on the Dynamic Coordination Control Algorithm of Braking Force for EV. Master's Thesis, Jilin University, Changchun, China, June 2013.



© 2017 by the authors. Licensee MDPI, Basel, Switzerland. This article is an open access article distributed under the terms and conditions of the Creative Commons Attribution (CC BY) license (<http://creativecommons.org/licenses/by/4.0/>).